

Phonon Lifetime Investigation of Anharmonicity and Thermal Conductivity of UO_2 by Neutron Scattering and Theory

Judy W.L. Pang,^{1,*} William J.L. Buyers,² Aleksandr Chernatynskiy,³ Mark D. Lumsden,⁴
Bennett C. Larson,¹ and Simon R. Phillpot³

¹Oak Ridge National Laboratory, Materials Science and Technology Division, Oak Ridge, Tennessee 37831, USA

²Chalk River Laboratories, National Research Council, Chalk River, Ontario, Canada K0J 1J0

³Department of Materials Science and Engineering, University of Florida, Gainesville, Florida 32611, USA

⁴Oak Ridge National Laboratory, Quantum Condensed Matter Division, Oak Ridge, Tennessee 37831, USA

(Received 6 October 2012; published 8 April 2013)

Inelastic neutron scattering measurements of individual phonon lifetimes and dispersion at 295 and 1200 K have been used to probe anharmonicity and thermal conductivity in UO_2 . They show that longitudinal optic phonon modes carry the largest amount of heat, in contrast to past simulations and that the total conductivity demonstrates a quantitative correspondence between microscopic and macroscopic phonon physics. We have further performed first-principles simulations for UO_2 showing semiquantitative agreement with phonon lifetimes at 295 K, but larger anharmonicity than measured at 1200 K.

DOI: [10.1103/PhysRevLett.110.157401](https://doi.org/10.1103/PhysRevLett.110.157401)

PACS numbers: 78.70.Nx, 63.20.dk, 63.20.Ry, 71.27.+a

As a fundamentally important $5f$ correlated electron system, understanding the vibrational, thermal, and electronic properties of uranium dioxide (UO_2) has been a strong priority experimentally and theoretically. Of particular importance for UO_2 as a nuclear fuel is an understanding of the underlying science of anharmonicity and its impact on phonon lifetimes and thermal conductivity. Despite the fact that anharmonicity of UO_2 represents a challenge at the forefront of many-body physics, neither experimental nor theoretical studies of phonon lifetimes exist for UO_2 . Phonon dispersion measurements are available for many materials; however, the corresponding phonon lifetime (i.e., inverse linewidth) measurements as a function of wave vector to study anharmonicity have been reported for only a handful of materials, including Al [1–3], K [4], (Na,K,Rb)-Cl [5], CaF_2 [6,7], and PbTe [8]. For insulating UO_2 , inelastic neutron scattering (INS) measurements of phonon dispersion by Dolling *et al.* [9] have been available since 1965, but the phonon lifetimes needed to address anharmonicity and thermal conductivity have not been measured.

The theoretical framework for anharmonicity and phonon lifetimes within perturbation theory [10,11] is well established. However, only recently have first-principles techniques become available for simulating phonon lifetimes and thermal conductivity. Success has been demonstrated in materials such as Al [3], Si [12,13], PbTe [14], and MgO [15]. While several first-principles phonon dispersion simulations have been reported for UO_2 [16–19], first-principles phonon lifetime simulations in strongly correlated materials present a significantly larger challenge [16,20] and have not been addressed so far.

Here, we present high-resolution inelastic neutron scattering measurements of phonon lifetimes and dispersion in UO_2 at 295 and 1200 K that form a benchmark dataset

against which advances in numerical simulations may be assessed. UO_2 is chosen as a first test of thermal conductivity because it is a classic example for theory dealing with correlated systems. We show by analysis that a longitudinal optic branch of phonons carries the largest amount of heat and comprises nearly one-third of the heat transport. We show that the total thermal conductivity from all phonons is in quantitative agreement with macroscopic thermal conductivity measurements. We further present first-principles simulations of phonon dispersion and lifetimes for UO_2 via 3rd order anharmonic calculations.

We recall that INS phonon measurements provide direct access to their lifetimes and group velocities as required for absolute experimental determinations of the phonon branch specific and total thermal conductivity in insulators. In the relaxation time approximation [10], the thermal conductivity $\kappa_{\mathbf{q}j}$ for phonons of wave vector \mathbf{q} and branch j is given by:

$$\kappa_{\mathbf{q}j} = \frac{1}{3} C_{\mathbf{q}j} v_{\mathbf{q}j} \lambda_{\mathbf{q}j} = \frac{1}{3} C_{\mathbf{q}j} v_{\mathbf{q}j}^2 \Gamma_{\mathbf{q}j}^{-1}, \quad (1)$$

where $C_{\mathbf{q}j}$ is the phonon heat capacity and $v_{\mathbf{q}j} = \frac{\partial E_{\mathbf{q}j}}{\partial \mathbf{q}}$ is the group velocity determined by local dispersion gradients. The phonon mean free paths $\lambda_{\mathbf{q}j} = v_{\mathbf{q}j} \tau_{\mathbf{q}j}$ depend on the measured phonon linewidths 2Γ (angular frequency) through the relaxation time $\tau_{\mathbf{q}j} = \Gamma_{\mathbf{q}j}^{-1}$ [10].

In general, phonon energy determinations such as the room temperature dispersion measurements for UO_2 [9] do not require high energy resolution. In this study, to ensure sufficient energy resolution for measurements of the linewidths and the energies, the spectrometer resolution was set to be smaller than the intrinsic phonon widths as described in the Supplemental Material [21]. Because of

the time-intensive nature of these comprehensive INS measurements, two temperatures of 295 K (~ 100 K below Debye temperature Θ_D [17]) and 1200 K ($3\times$ the Θ_D and close to reactor operating temperatures) were selected.

Figure 1(a) shows the phonon dispersion measurements in which the six observable branches in the (*HHL*) scattering plane were measured along the 3 main symmetry directions. The nine phonon branches for the UO_2 cubic-fluorite primitive cell include transverse acoustic (TA) modes taken to be double-degenerate, a longitudinal acoustic (LA) mode, two doubly-degenerate transverse optic (TO1 and TO2) modes, and two longitudinal optic (LO1 and LO2) modes along the [001](Δ), and [111](Λ) directions; the phonon space-group representation is given in parentheses. For the [110](Σ) direction the structure factors vanish for three distinct transverse branches with polarization vectors perpendicular to the scattering plane.

The phonon dispersion measurements at 295 K given in Fig. 1(a) are in excellent agreement with the (lower resolution) historic results of Dolling *et al.* [9]. The measurements made at 1200 K represent the only dispersion curve measurements for UO_2 at high temperature; phonon energy measurements at a few selected wave vectors above 1600 K were reported elsewhere [22,23].

The grey lines in Fig. 1(a) are piecewise fits to the phonon energies measured at 1200 K to facilitate the computation of group velocities and constrain the velocities (i.e., gradients) to vanish at zone boundaries as required by symmetry. The relatively small energy softening with temperature shows that the group velocities change little with temperature.

The phonon peak spectra at 295 and 1200 K in Figs. 1(b)–1(e) show examples of the procedure used to generate the dispersion data in Fig. 1(a). The phonon energies and intrinsic (i.e., resolution corrected) linewidths (2Γ) were extracted by least squares fitting the measured phonon spectra to a Lorentzian convoluted with the known 4D spectrometer resolution function [24] for planar dispersion.

The intrinsic full widths at half maximum, 2Γ , for all measured phonons (58 at 295 K and 86 at 1200 K) are plotted in Fig. 2. Noticing that the phonon linewidths more than double from 295 to 1200 K, we expect from a corresponding $2\text{--}3\times$ decrease in thermal conductivity [Eq. (1)] since the velocities are essentially constant. Considering that the standard deviations (1%–10%) of the widths are smaller than the symbol size in most cases, the nonmonotonic q dependence of the linewidths in Fig. 2 is considered significant. It may arise from the conservation of momentum and energy limitations on the phase space available for phonon decays into two-phonon states [11,25].

Quasiharmonic simulations were made to calculate the phonon dispersion and linewidths [26] in a $13 \times 13 \times 13$

q -points cubic Brillouin zone mesh for UO_2 at 295 and 1200 K using generalized gradient approximation with Hubbard- U correction (GGA + U) [27]. The lattice constants obtained by free energy minimization were 5.569 Å at 295 K and 5.637 Å at 1200 K, which are $\sim 2\%$ above experimental values [17]. A $2 \times 2 \times 2$ supercell was used to determine the interatomic forces via the projector augmented wave pseudopotential method [28] with an energy cutoff of 500 eV using VASP [29]. The 2nd and 3rd order interatomic force constants [11] required to determine phonon energies and lifetimes were obtained by numerical

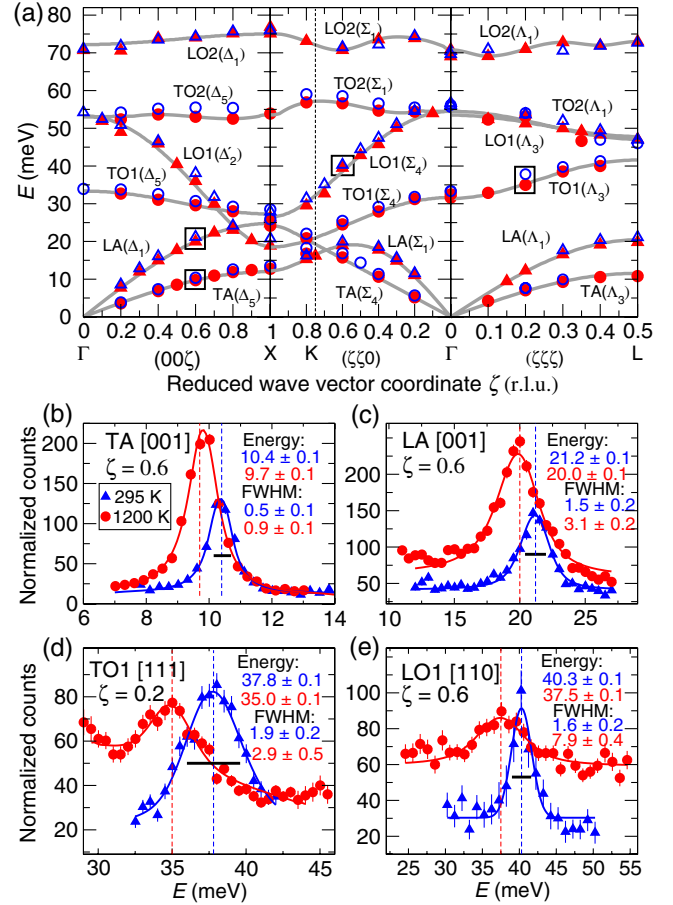


FIG. 1 (color online). (a) Dispersion curves measurements for UO_2 at 295 and 1200 K in directions [001], [110], and [111]. The circles (triangles) represent transverse (longitudinal) phonons and the blue solid (red open) symbols denote measurements at 295 (1200) K. The grey lines in (a) are piecewise fits to the data at 1200 K as a guide to the eye. ζ is the wave vector in reciprocal lattice units (r.l.u.) of $\frac{2\pi}{a}$ where a is the lattice parameter. (b)–(e) Examples of neutron scattering energy scans at constant- Q for (b) TA, (c) LA, (d) TO1, and (e) LO1 phonons at 295 K (blue triangles) and 1200 K (red circles). The four black squares on panel (a) indicate the position of the (b)–(e) measurements. The panels (b)–(e) illustrate how phonon energies and intrinsic linewidths are obtained from resolution-convoluted Lorentzian fitting of the peaks (solid lines). The instrumental linewidths are shown by horizontal black lines.

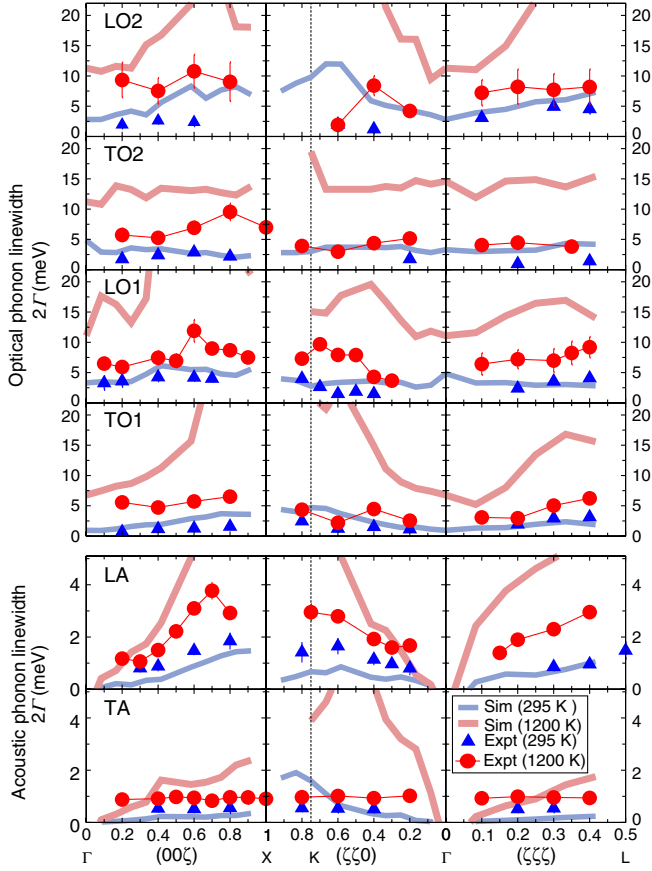


FIG. 2 (color online). Measured intrinsic phonon linewidths 2Γ for UO_2 at 295 K (blue triangles) and 1200 K (red circles with connecting lines) in the [001], [110], and [111] directions for the TA, LA, TO1, LO1, TO2, and LO2 phonon branches. Standard deviation error bars are visible for the LO1 and LO2 branches of the 1200 K data; the uncertainties are smaller than the symbols for most other points. The thick light blue and light red lines represent quasi-harmonic phonon linewidth simulations performed in this study using GGA + U for 295 and 1200 K, respectively.

differentiation under finite displacements of the atoms in the supercell as described previously [15]. The ideal cubic structure with antiferromagnetic spin arrangements was used throughout the calculations and the electrostatic contribution was accounted for as described by Wang *et al.* [30] and Nunes *et al.* [31]. To ensure the same minimum of the system under atomic displacements, the occupation matrix of the $5f$ electrons was fixed to the ground state during the first 25 steps of the self-consistent field calculations in the numerical differentiation.

The simulated phonon energies are compared with the INS measurements in Fig. 3. Agreement is good for the acoustic TA and LA phonons and also for the highly dispersive longitudinal optic LO1 phonons. The energies for the TO1, TO2, and LO2 optic phonons differ by somewhat larger amounts, a characteristic observed in other first-principles simulations for UO_2 [17–19] as well.

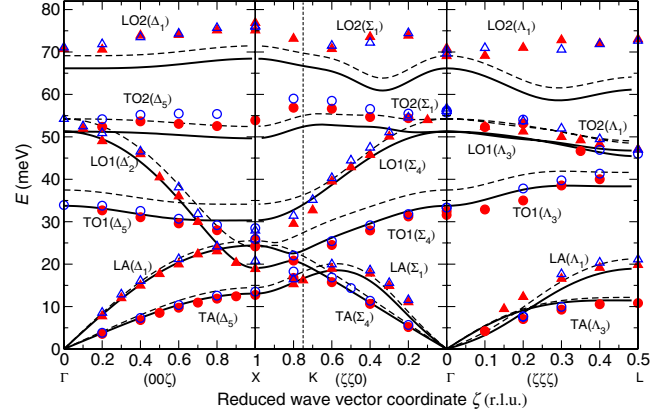


FIG. 3 (color online). Simulations of phonon dispersion for UO_2 at 295 (dotted lines) and 1200 K (solid lines) using GGA + U compared with the INS measurements of dispersion of Fig. 1.

The GGA + U simulated phonon linewidths are plotted as thick blue and red lines in Fig. 2. The agreement between the simulated linewidths and INS measurements at 295 K is semiquantitative, with a tendency to underestimate the widths for acoustic modes and to overestimate the widths for the highest energy LO2 optic modes. For 1200 K, the simulations strongly overestimate the linewidths for both the acoustic and optic modes. Some of the simulated phonons are overdamped in contrast to the moderate anharmonic effects observed in the INS phonon spectra which are well defined. The energy scales in Fig. 2 were allowed to truncate the largest simulated linewidths at 1200 K in order to display the 295 K data clearly.

We now connect the microscopic phonon dispersion and linewidth measurements directly with macroscopic thermal conductivity for UO_2 by integrating Eq. (1) over the Brillouin zone. The branch specific and total thermal conductivities in Fig. 4 were obtained directly from the INS measurements by weighting the [001], [011], or [111] phonon data according to their respective solid angles within the Brillouin zone (see Supplemental Material [21]) and assuming angular isotropy around each symmetry direction.

Our results are in stark contrast to recent arguments based on a dynamical mean field theory analysis [16] that the LA branch is the only significant carrier of heat. Instead, we have shown that the (high velocity) LO1 phonons transport the largest amount of heat in cubic-fluorite UO_2 [Fig. 4(a)]. The INS measurements show that the contribution from the LO1 optic phonons is strong because their high velocities more than compensate for their larger linewidths. The weak contributions by the TO2 and LO2 optic branches are the result of low velocities and short lifetimes. The 1200 K results in Fig. 4 show large thermal conductivity decreases for all phonon branches as a result of temperature broadened linewidths. The TO1 and LO1 optic mode thermal conductivities are observed to decrease more than the acoustic phonons;

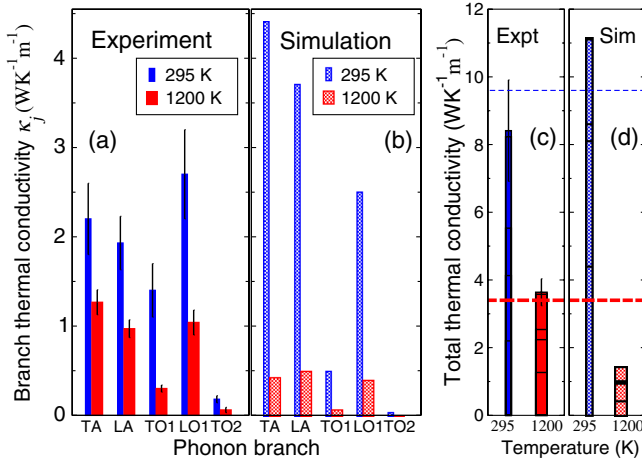


FIG. 4 (color online). Measured and simulated branch specific thermal conductivity at 295 K (thin blue) and 1200 K (thick red): (a) from INS measurements; (b) from GGA + U simulations; (c),(d) total thermal conductivities obtained by INS measurements and GGA + U simulations. The thin black vertical lines in (a) and (c) are the experimental uncertainties; the thin and thick dashed horizontal lines in (c) and (d) denote the macroscopic thermal conductivities for UO₂ at 295 and 1200 K, respectively [32]; the double degeneracy of transverse modes is included in the plots. The LO2 phonon conductivity is too small to display.

however, even at 1200 K the LO1 branches transport a surprisingly large 30% fraction of the total heat.

The total thermal conductivities in Fig. 4(c), obtained by integrating the individual branch conductivities are to be compared directly with the macroscopic thermal conductivities of UO₂. The INS measured integral values of $8.4 \pm 1.5 \text{ W m}^{-1} \text{ K}^{-1}$ at 295 K and $3.6 \pm 0.4 \text{ W m}^{-1} \text{ K}^{-1}$ at 1200 K are in good agreement with the respective macroscopic thermal conductivities [32] of $9.7 \text{ W m}^{-1} \text{ K}^{-1}$ and $3.4 \text{ W m}^{-1} \text{ K}^{-1}$ given by the dashed horizontal lines in Fig. 4(c). This is an important demonstration of the quantitative experimental correspondence between microscopic and macroscopic phonon physics in UO₂.

The benchmark phonon lifetime and dispersion measurements presented here provide a unique opportunity for confronting the thermal conductivity predictions of GGA + U or new theories with INS measurements on a common basis. And to that end, we show in Fig. 4(b) simulated branch specific thermal conductivities determined using the same Brillouin zone integration procedure as used for the INS measurements of Fig. 4(a). The GGA + U simulations predict, at 295 K, higher acoustic mode and lower optic mode conductivities than the INS measurements because of the lower acoustic and higher optic mode linewidth predictions. We note, however, that the LO1 phonon branch is predicted to have strong thermal conductivity, in agreement with experiment. Although the total conductivity at 295 K of $11.1 \text{ W m}^{-1} \text{ K}^{-1}$ from the simulation is within 15% of the macroscopic value for UO₂, the INS linewidth benchmarks indicate that the close

agreement is due in part to offsetting errors in the acoustic and optic mode conductivities.

Because the simulated linewidths for all phonon branches at 1200 K are much larger than the measurements at 1200 K, all the simulated branch-specific conductivities show dramatically stronger decreases with temperature than are measured by INS. As a result, the GGA + U predicted total conductivity at 1200 K of $1.4 \text{ W m}^{-1} \text{ K}^{-1}$ [Fig. 4(d)] is less than half of the macroscopic measured value. As with the 295 K result, the prediction of roughly one-third of the heat being transported by each of the TA, LA, and the LO1 phonon branches is in qualitative agreement with the INS experimental benchmarks.

Now, these phonon lifetime measurements and the extraction of quantitative branch specific thermal conductivities have important implications for probing anharmonicity. Figure 2 indicates that phonon linewidths provide a much more sensitive test of anharmonicity than do the energy dispersion measurements in Fig. 3.

The direct confrontation of first-principles anharmonic lattice dynamics simulations with INS measurements of phonon lifetimes makes possible a new level of specificity in anharmonicity investigations. Moreover, preliminary tests (1) using the 295 K phonon energies in 1200 K lifetime simulations and (2) using the 295 K 3rd order interatomic force constants in 1200 K lifetime simulations have been performed. These tests show that the simulated phonon lifetimes for 1200 K in Fig. 2 are ~ 3 – 5 times more sensitive to the interchange of the phonon energies and produce better agreement with measurements than interchanging the 3rd order interatomic force constants. This underscores the importance of electronic structures that produce highly accurate 2nd order, as well as 3rd order, force constants to simulate phonon lifetimes.

To address the observed discrepancies with INS lifetime measurements in the near term, there are potential improvements in our GGA + U approach that should be considered, such as the inclusion of spin-orbit interactions with Hubbard- U and the minimization of the known spurious self-interaction effects on the strongly localized $5f$ electrons [33].

In addition, the use of more powerful theoretical approaches such as hybrid functional density functional theory [34] and dynamical mean field theory [16] represents an important direction for future simulations. However, the significantly higher computational requirements for such approaches have so far precluded their ability to address 3rd order anharmonicity.

Overall, the value of the phonon lifetime and dispersion measurements presented here have been demonstrated by direct comparison with our first-principles simulations in this technologically important strongly correlated system.

The authors are grateful to Mark Paffett of the Los Alamos National Laboratory for the loan of a 40 g UO₂ single crystal. A 90 g UO₂ crystal was supplied by our author W.J.L.B. We thank Brent Taylor, Michael

Trammell, and Curtis Maples of Oak Ridge National Laboratory (ORNL) for technical support on experimental preparation. We thank Boris Dorado of CEA, France for technical assistance and valuable discussions on the simulations. Research at ORNL was sponsored by the U.S. Department of Energy (DOE), Office of Basic Energy Sciences (BES), CMSNF, an Energy Frontier Research Center (EFRC). A. C. and S. R. P. are subcontractors of the U.S. Government under Contract No. DE-AC07-05ID14517, under the CMSNF EFRC (Office of Science, BES, FWP 1356). The Research at ORNL High Flux Isotope Reactor was sponsored by the Scientific User Facilities Division of BES. W. J. L. B. acknowledges the Canadian Institute for Advanced Research.

*pangj@ornl.gov

- [1] R. Stedman and G. Nilsson, *Phys. Rev.* **145**, 492 (1966).
- [2] W. J. L. Buyers, G. Dolling, G. Jacucci, M. L. Klein, and H. R. Glyde, *Phys. Rev. B* **20**, 4859 (1979).
- [3] X. Tang, C. W. Li, and B. Fultz, *Phys. Rev. B* **82**, 184301 (2010).
- [4] W. J. L. Buyers and R. A. Cowley, *Phys. Rev.* **180**, 755 (1969).
- [5] G. Raunio, *Phys. Status Solidi B* **35**, 299 (1969).
- [6] K. Schmalzl, D. Strauch, and H. Schober, *Phys. Rev. B* **68**, 144301 (2003).
- [7] M. Iizumi, *J. Phys. Soc. Jpn.* **35**, 204 (1973).
- [8] O. Delaire, J. Ma, K. Marty, A. F. May, M. A. McGuire, M. H. Du, D. J. Singh, A. Podlesnyak, G. Ehlers, M. D. Lumsden, and B. C. Sales, *Nat. Mater.* **10**, 614 (2011).
- [9] G. Dolling, R. A. Cowley, and A. D. B. Woods, *Can. J. Phys.* **43**, 1397 (1965).
- [10] A. A. Maradudin and A. E. Fein, *Phys. Rev.* **128**, 2589 (1962).
- [11] R. A. Cowley, *Rep. Prog. Phys.* **31**, 123 (1968).
- [12] D. A. Broido, M. Malorny, G. Birner, N. Mingo, and D. A. Stewart, *Appl. Phys. Lett.* **91**, 231922 (2007).
- [13] A. Ward and D. A. Broido, *Phys. Rev. B* **81**, 085205 (2010).
- [14] Z. Tian, J. Garg, K. Esfarjani, T. Shiga, J. Shiomi, and G. Chen, *Phys. Rev. B* **85**, 184303 (2012).
- [15] X. Tang and J. Dong, *Proc. Natl. Acad. Sci. U.S.A.* **107**, 4539 (2010).
- [16] Q. Yin and S. Y. Savrasov, *Phys. Rev. Lett.* **100**, 225504 (2008).
- [17] M. Sanati, R. C. Albers, T. Lookman, and A. Saxena, *Phys. Rev. B* **84**, 014116 (2011).
- [18] Y. Yun, D. Legut, and P. M. Oppeneer, *J. Nucl. Mater.* **426**, 109 (2012).
- [19] B.-T. Wang, P. Zhang, and O. Eriksson, [arXiv:1201.5003](https://arxiv.org/abs/1201.5003).
- [20] G. Kotliar (private communication).
- [21] See Supplemental Material at <http://link.aps.org/supplemental/10.1103/PhysRevLett.110.157401> for details of the experimental setup and the Brillouin zone integration.
- [22] K. Clausen *et al.*, *High Temp. Sci.* **19**, 189 (1985).
- [23] M. T. Hutchings, *J. Chem. Soc., Faraday Trans. 2* **83**, 1083 (1987).
- [24] A. Zheludev, “Reslib,” <http://www.neutron.ethz.ch/research/resources/reslib>.
- [25] L. Lindsay and D. A. Broido, *J. Phys. Condens. Matter* **20**, 165209 (2008).
- [26] A. Chernatynskiy and S. R. Phillpot, *Phys. Rev. B* **82**, 134301 (2010).
- [27] S. Dudarev, D. Manh, and A. Sutton, *Philos. Mag. B* **75**, 613 (1997).
- [28] P. E. Blochl, *Phys. Rev. B* **50**, 17953 (1994).
- [29] G. Kresse and J. Hafner, *Phys. Rev. B* **47**, 558 (1993); **49**, 14251 (1994); G. Kresse and J. Furthmuller, *Phys. Rev. B* **54**, 11169 (1996); *Comput. Mater. Sci.* **6**, 15 (1996).
- [30] Y. Wang, J. J. Wang, W. Y. Wang, Z. G. Mei, S. L. Shang, L. Q. Chen, and Z. K. Liu, *J. Phys. Condens. Matter* **22**, 202201 (2010).
- [31] R. W. Nunes and X. Gonze, *Phys. Rev. B* **63**, 155107 (2001).
- [32] G. J. Hyland, *J. Nucl. Mater.* **113**, 125 (1983).
- [33] F. Zhou and V. Ozoliņš, *Phys. Rev. B* **80**, 125127 (2009).
- [34] K. N. Kudin, G. E. Scuseria, and R. L. Martin, *Phys. Rev. Lett.* **89**, 266402 (2002).